Carbohydrate Research, 227 (1992) 73–83
Elsevier Science Publishers B.V., Amsterdam

The influence of chain length on the hydrodynamic behaviour of amylose*

Philippe Roger† and Paul Colonna
Institut National de la Recherche Agronomique, Rue de la Géraudière, B.P. 527, 44026 Nantes 03 (France)

(Received January 18th, 1991; accepted for publication April 17th, 1991)

ABSTRACT

Dilute aqueous solutions of amylose (<1.5 mg/mL) have been studied by static and dynamic light-scattering techniques. The samples used were monodisperse fractions which covered molecular weights in the range $2 \times 10^4 - 1 \times 10^6$. The hydrodynamic radii (R_H) were computed from the translational diffusion coefficient at infinite dilution. The characteristic exponents for the dependence of the molecular weight on the dimensions of the polymer chain in good solvents, determined as ν_G for R_G values and ν_H for R_H values, respectively, were close to the value predicted for a θ solvent in 0.1M KCl (ν_H 0.47, ν_G 0.51) and for a good solvent in 0.1M KOH (ν_H 0.57, ν_G 0.67). The ratio $\xi = R_H/R_G$ is discussed, as is the stiffness of the polymer in those solvents on the basis of the persistence length.

INTRODUCTION

There have been relatively few investigations of the hydrodynamic properties of amylose, a (1→4)-α-D-glucan[1,2], especially in aqueous solutions where retrogradation tends to occur spontaneously.

Light scattering is the only technique that allows the complete characterisation of a polymer in solution[3]. It has been concluded[1,4–8] that amylose behaves as a non-free-draining coil. However, there are discrepancies between the values reported for the stiffness of the polymer chain (characteristic ratio and persistence length). Two models have been proposed for the conformation of amylose in solution. The first[9] involves a random coil without helical character for solutions in alkali and methyl sulfoxide, and the second[10], for neutral solutions, a relatively stiff helix, interpersed by short regions of random coil. However, the latter conformation cannot be observed by static light-scattering and only methods with large values of the scattering vector $\mathbf{k} = 4\pi/\lambda \sin \theta/2$, such as small-angle X-ray scattering (SAXS), are sufficiently powerful. Braga *et al.*[11] studied a carboxymethylamylose with a low d.s. (0.08) by SAXS and found a mass per unit length (M_u) of ~ 140 Da.Å^{-1}, which is nearer to that (162 Da.Å^{-1}) computed for the compact V helix than that (40 Da.Å^{-1}) calculated for the stretched conformation. The helical character of amylose in aqueous solution has been supported by studies of molecular modeling. Thus, amylose chains should be highly disordered in solution, but

* Dedicated to Professor David Manners.
† To whom correspondence should be addressed.

0008-6215/92/$ 05.00

with discernible sequences of short-range helical structures which are irregular and labile[12,13].

All these conclusions are inconsistent. Most investigations were carried out on polydisperse ($d.p._n/d.p._w$ 2–4) materials[4,5,7,8] or preparations with high molecular weights[1], or in strong solvents where the primary structure of the amylose may be destroyed. Only Huseman *et al.*[6] characterised enzymically synthesised amylose by static light-scattering, whereas others[4,9] sub-fractionated linear amylose in order to obtain fractions with a narrow range of molecular weights.

The present study concerns the persistence length of amylose in 0.1M KCl and KOH. Static and dynamic light-scattering (s.l.s. and d.l.s., respectively) methods applied to monodisperse fractions of amylose should allow the influence of the chain length to be studied.

EXPERIMENTAL

Monodisperse samples of amylose were synthesised[14] using maltoheptaose as a primer, D-glucose 1-phosphate, and potato phosphorylase (EC 1.2.4.1.1).

The fractions (10–80 mg) were each dispersed in M KOH (5 mL) and stirred gently for 16 h at 4°. Solutions in 0.1M KCl (A1–A5) were obtained by neutralising with M HCl and diluting to 100 mL with triply distilled and filtered water. All these operations were carried out in <30 min and the solutions were studied immediately. Solutions in 0.1M KOH (B1–B4) were prepared in a similar way in M KOH, then diluted. The concentrations were in the range 0.2–1.5 g/L. Solutions were directly filtered into cylindrical Burchard cells, using 0.45-μm ACRO LC3A and ACRO LC3S (Gelman®) filters. Concentrations were checked by the sulfuric acid-orcinol method[15].

Scattering experiments were performed at 25° in the range 10–145° in the homodyne mode with full photon-counting detection and a 128-channel K7025 Malvern correlator. Incident radiation at 514.5 nm was obtained from a 3-W Ar Ion Spectra-Physics laser and was vertically polarised. All fitting and monitoring programs were written in BASIC and run on a HP9300 microcomputer. Optical alignment was checked over the angular range 10–150° using filtered benzene. For d.l.s. measurements, after an accumulation for 100 s, data were treated using the method of cumulants[16]. For s.l.s. experiments, photons were counted during 100 s in order to obtain one point of the Zimm plot[17].

All other experimental methods have been described[18].

RESULTS

Amylose fractions were synthesised using potato phosphorylase, maltoheptaose, and D-glucose 1-phosphate as detailed in Table I. The main problem encountered was the instability of the amylose, which resulted in polydisperse and retrograded macromolecules. Therefore, syntheses were conducted on small batches, and small fractions (55–81 mg) were recovered for each molecular weight synthesised. Conversion levels of D-glucose 1-phosphate into amylose were in the range 55–68%. Linearity was confirmed

TABLE I

Phosphorylase-catalysed synthesis of amylose fractions

Fraction	*Maltoheptaose (mg)*	*Dipotassium D-glucose 1-phosphate (mg)*	*Time of incubation (h)*	*Yield of amylose (mg)*	*Conversion of D-glucose 1-phosphate into amylose (%)*
A1	3.333	250	1	71	59
A2	0.220	250	6	81	68
A3	0.220	250	16	76	63
A4	0.220	250	24	66	55
A5	0.220	250	24	79	66
B1	0.176	200	6	65	68
B2	0.176	200	16	58	61
B3	0.176	200	24	58	60
B4	0.176	200	24	55	58

by complete degradation with beta-amylase. Size-exclusion chromatography on Sepharose CL-2B in 0.1M KOH revealed a single sharp peak for each fraction, of the same width as for proteins (Fig. 1). In contrast, retrograded amylose gave bimodal or broad chromatograms (Fig. 1). Only the former samples were studied by light scattering.

Zimm plots (Fig. 2) were used to determine the apparent molecular weights, second virial coefficients A_2, and radii of gyration $<R_G^2>^{1/2}$, according to

$$\lim_{\substack{\mathbf{k}\to 0 \\ c\to 0}} \left(\frac{Kc}{\Delta R_\theta}\right) = \left(\frac{1}{M_p} + 2A_2c\right)\left(1 + \frac{\mathbf{k}^2 < R_G^2}{3}\right)$$

$$K = \frac{4\pi^2}{\lambda_0^4 N_A} n_0 \left(\frac{dn}{dc}\right)^2$$

$$\mathbf{k} = \frac{4\pi n_0}{\lambda_0} \sin\left(\frac{\theta}{2}\right),$$

where $\mathbf{k}$ is the magnitude of the scattering vector, λ is the wavelength of the light, n_0 is the refractive index of the solvent, dn/dc is the refractive index increment, and N_a is Avogadro's number. The optical constant K contains the wavelength λ_0 of incident light *in vacuo* and the square of dn/dc.

The literature values of dn/dc for amylose in aqueous solvents at 546 and 436 nm are given by Huglin[19], and Greenwood and Hourston[20], respectively. The differences between the values at these two wavelengths are <2%. Therefore, the values for 514.5 nm were considered to be identical to those at 546 nm (0.146 mL.g^{-1}). The accuracy of s.l.s. has been estimated at 5 and 10% for molecular weight and R_G, respectively, and 5–12% for A_2 measurements.

The results are summarised in Tables II and III. The $<R_G^2>^{1/2}$ for sample A1 was

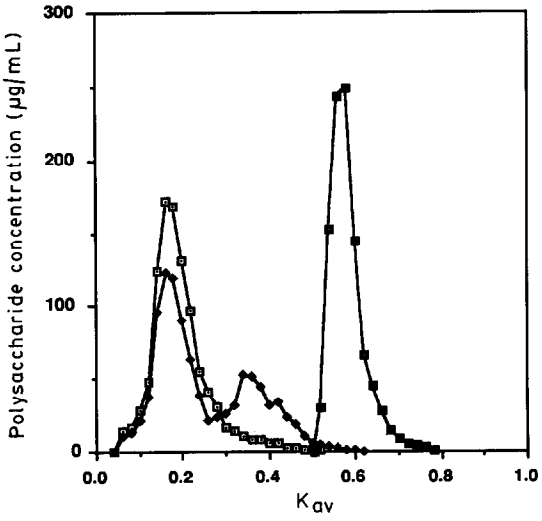

Fig. 1. Size-exclusion chromatography of samples of amyloses on Sepharose 2B-CL: A2 (■) and A4 (⊡), and a discarded sample (◆) obtained under the same conditions as A4.

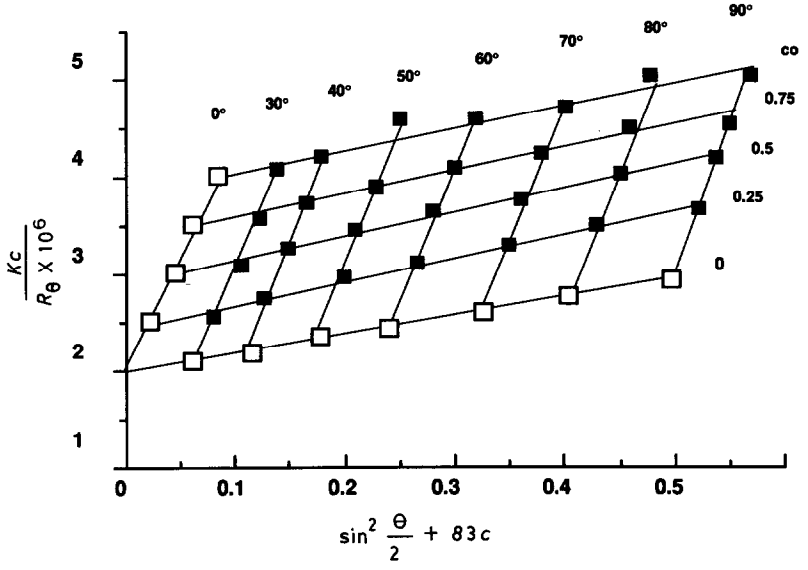

Fig. 2. Zimm plot obtained for amylose fraction B4 in 0.1M KOH at 25°, c_o = 0.806 g/L, *dn/dc* = 0.146 mL/g, λ = 514.5 nm.

not reported due to a large uncertainty in the angular dependence data caused by dust. Difficulties occurred for the fraction of higher molecular weight because solutions of A5 were difficult to filter. The molecular weights of fractions studied in 0.1M KCl ranged from 2×10^4 to 1×10^6 g/mol and 1.7×10^5 to 8×10^5 g/mol for those in 0.1M KOH. Second virial coefficients A_2 were greater in 0.1M KOH (in the range 10^{-3} mol/g) than in

TABLE II

Static and dynamic results on amylose fractions with 0.1M KCl as the solvent

Fraction	$M_w \times 10^{-5}$	$A_2 \times 10^3$ (*mol. cm³.g⁻²*)	$\langle R_G^2 \rangle_z^{1/2}$ (*nm*)	$\langle R_H^2 \rangle_z^{1/2}$ (*nm*)	$\langle R_H^2 \rangle_z^{1/2} / \langle R_G^2 \rangle_z^{1/2}$
A1	0.2	0.104	n.d.[a]	5	–
A2	1.7	1.404	21	13.5	0.643
A3	4.2	0.045	33	22	0.667
A4	7.4	0.031	45	28	0.622
A5	10.0	0.099	51	31	0.608

[a] Not determined.

TABLE III

Static and dynamic results on amylose fractions with 0.1M KOH as the solvent

Fraction	$M_w \times 10^{-5}$	$A_2 \times 10^3$ (*mol.cm³.g⁻²*)	$\langle R_G^2 \rangle_z^{1/2}$ (*nm*)	$\langle R_H^2 \rangle_z^{1/2}$ (*nm*)	$\langle R_H^2 \rangle_z^{1/2} / \langle R_G^2 \rangle_z^{1/2}$
B1	1.7	1.790	28	16	0.571
B2	4.0	1.320	46	24	0.522
B3	5.0	1.109	57	26	0.456
B4	8.0	0.592	80	40	0.500

0.1M KCl where they decreased to 10^{-4}–10^{-5} mol/g. One fraction A2 presented a high value for A_2 (1.404×10^{-3} mol.cm³.g^{-2}). The same tendency was observed for the radius of gyration which ranged from 21 to 51 nm in 0.1M KCl and from 28 to 80 nm in 0.1M KOH.

D.l.s. gave the translational diffusion coefficient D for one angle and one concentration, with sample times varying from 1 to 15 μs. Fig. 3 shows a typical second-order autocorrelation function and the theoretically fitted third-order polynomial on the right with standard deviation between experimental and fitted values, and the logarithm of these functions on the left. After extrapolation to zero concentration and zero angle, D followed the Stokes–Einstein relation

$$\lim_{\substack{k\to 0 \\ c\to 0}} D = \frac{k_B T}{6\pi \eta_s R_H},$$

where k_B is Boltzmann's constant, T is the absolute temperature, and η_s is the viscosity of the solvent.

The hydrodynamic radii R_H, calculated from the Stokes–Einstein equation, using the viscosities of 0.1M KCl and 0.1M KOH, respectively, are listed in Tables II and III. R_H ranged from 5 to 40 nm with generally greater values in 0.1M KOH than in 0.1M KCl. The experimental precision for the hydrodynamic radius determination was ~ 10%.

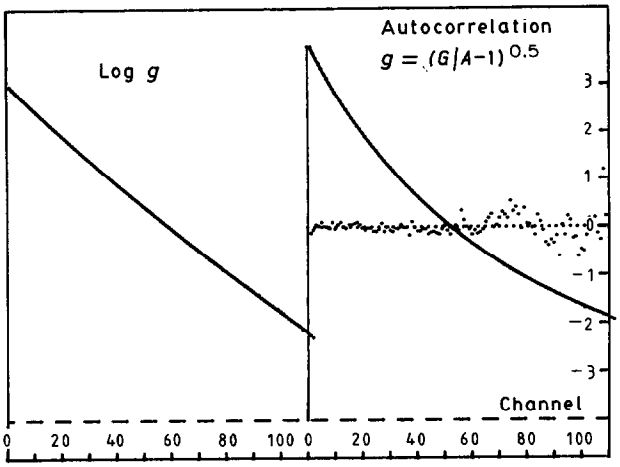

Fig. 3. Autocorrelation function g (after baseline normalisation of the experimentally determined quantity, G, and taking the square root of the remaining self-beat function), log g, and standard deviation between experimental and fitted values *vs.* channel number for amylose fraction B2 in 0.1M KOH: c = 0.789 g/L, scattering angle θ = 30°, sample time τ = 20 μs.

The angular dependence function D was linear at $\theta < 90°$. This result accords with the relationship that characterises the regime where the signal due to translational diffusion is adequately separated in frequency from rotational and flexing modes which occur on shorter time scales, *i.e.*, $\mathbf{k} < R_G^2 >_z < 1$.

DISCUSSION

Small batches of amylose were recovered, due to the limited amount (~ 180 U) of potato phosphorylase purified. Although the preparation of the enzyme from potatoes is straightforward, the procedure is long and tedious. Therefore, characterisation of these fractions was limited to size-exclusion chromatography. Synthetic amyloses are linear and the chromatographic behaviour of the various fractions suggested that they were nearly monodisperse. No calibration of the column was carried out, as peak broadening due to axial dispersion is important in low-pressure chromatographic systems[21].

The samples covered a range of molecular weights over two decades and enabled the influence of molecular weight on conformation to be studied. Two different solvents were used in order to study the expansion effects. The hydrodynamic radius R_H, determined by d.l.s., is related to the radius of gyration R_G by a proportionality constant ξ: $R_H = \xi R_G$, and ξ for a monodisperse linear chain in the unperturbed state has been discussed[22]; ξ has a theoretical value of 0.665 in θ solvents and of 0.537 in good solvents[23]. 0.33M KCl is a θ solvent for amylose[4]. In 0.1M KCl, ξ was in the range 0.608–0.667, *i.e.*, up to 10% lower than the value expected for a θ solvent. Such a discrepancy has been observed for other systems such as polystyrene in *trans*-decahydronaphthalene[24]. In contrast, 0.1M KOH, which is commonly used for dispersing

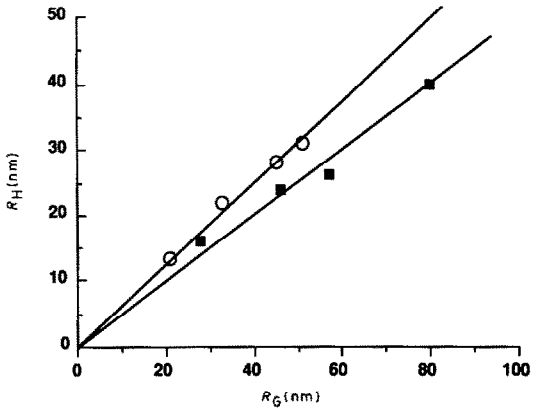

Fig. 4. Hydrodynamic radius versus gyration radius for amyloses in 0.1M KCl (o) and in 0.1M KOH (■).

amylose, gave values of A_2 and ξ (0.571–0.456) (Tables II and III) characteristic of a good solvent. Fig. 4 shows the variation of R_H versus R_G (ξ_{KCl} = 0.613 and ξ_{KOH} = 0.483), which confirmed the previous discussion.

For a polymer with a sufficiently high molecular weight, the dimensions of the chain extrapolated to infinite dilution depend on the molecular weight as a simple power law: $R_G \sim M^{\nu_G}$ and $R_H \sim M^{\nu_H}$.

The characteristic exponents, ν_G and ν_H, are of interest both experimentally and theoretically. The consistency between the values of ν_G and ν_H was predicted by Flory[25] in terms of non-draining chain concepts and also by de Gennes[26]. The theoretical values at the asymptotic limit of the excluded-volume effect are $\nu = 0.6$ in Flory's theory and $\nu = 0.588$ in the renormalisation calculation[27]. The analysis of molecular weight versus hydrodynamic or gyration radii gives further information on the quality of the solvent. In the relation $R \sim M^{\nu}$, $\nu = 3/5$ (or so) in good solvents and $\nu = 1/2$ in θ solvents[27]. The dependence of R_G and R_H on molecular weight is shown in Fig. 5 on a log-log scale. The values are close to theoretical $\nu_H = 0.49$ ($r = 0.987$) and $\nu_G = 0.51$ ($r = 0.934$) for 0.1M KCl, and $\nu_H = 0.57$ ($r = 0.937$) and $\nu_G = 0.67$ ($r = 0.864$) for 0.1M KOH.

Hydrodynamic behaviour and molecular stiffness may be determined by analysing[8] the dependence of $<R_H^2>_z$ and $<R_G^2>_z$ on molecular weight $<M_w>$.

$<R_G^2>_z = K_\alpha <M_w>^\alpha$

$<R_H^2>_z = K_\gamma <M_w>^\gamma$

For amylose in 0.1M KCl and 0.1M KOH, the respective coefficients α, γ, K_α, and K_γ are listed in Table IV. For 0.1M KCl, α is 1.01 and γ is 0.95. These results confirmed that in dilute, neutral aqueous solution, amylose behaves as a non-free draining coil, with a conformation characterised[1] by $\alpha = \gamma = 1$.

In Me_2SO, aqueous KOH, and aqueous NaOH as solvents, amylose behaves as an "interrupted helix" in which the molecule has long helical sections with short interpersed regions of random coil[1]. The latter regions confer the flexibility necessary for the macromolecule to conform to the random coil model, which explains why α and γ are greater for amylose in 0.1M KOH (1.35 and 1.13, respectively) than in 0.1M KCl (Table IV).

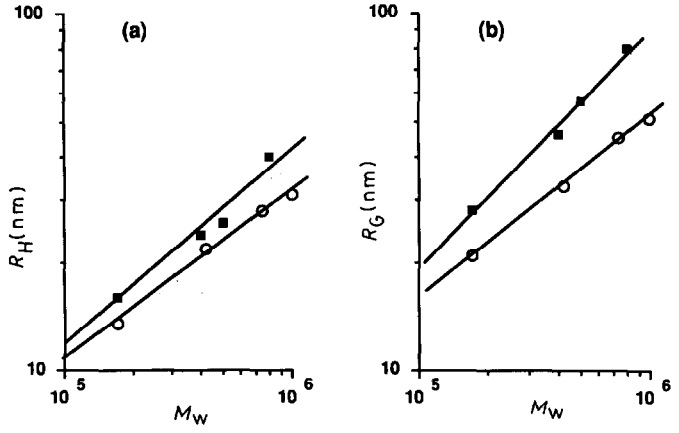

Fig. 5. Variation in hydrodynamic (a) and gyration (b) radii *vs.* molecular weight in 0.1M KOH (■) and 0.1M KCl (○).

TABLE IV

Determination of the respective coefficients α, γ, K_α, and K_γ[a] for amylose in 0.1M KCl and 0.1M KOH

Solvent	α	K_α *(m²/Da)*	r	γ	K_γ *(m²/Da)*	r
0.1M KCl	1.01	2.19×10^{-21}	1.00	0.95	2.10×10^{-21}	0.99
0.1M KOH	1.35	6.42×10^{-23}	0.99	1.13	2.71×10^{-22}	0.95

[a] In the relations $<R_G^2>_z = K_\alpha <M_w>^\alpha$ and $<R_H^2>_z = K_\gamma <M_w>^\gamma$ with the respective correlation coefficient of the linear regression *r*.

Weill and des Cloizeaux[29] deduced the relation $[\eta] \sim R_G^2 R_H/M$ for the intrinsic viscosity, using the blob concept. Substitution of the observed values in this relationship gives the theoretical exponents $\alpha = 0.488$ in 0.1M KCl and 0.92 in 0.1M KOH in the Mark–Houwink relationship, $[\eta] \sim M^\alpha$. These calculated values are in good agreement with the observed[1] exponents $\alpha = 0.5$ in 0.33M KCl and 0.78 in 0.2M KOH. Therefore, the discrepancies between ν_H and ν_G can be explained by the blob concept.

In comparing the intrinsic extension of chains with different d.p., it is useful to consider the dimensionless quantity C_∞ (the characteristic ratio) generally defined as the ratio between the dimension of real and freely jointed chains[30]:

$$C_\infty = \frac{6\langle R_G^2\rangle_w}{\langle n\rangle_w I_0^2} = \frac{6\langle R_G^2\rangle_z}{\langle n\rangle_z I_0^2},$$

where I_0 is the projected length of the glucosyl unit and $<n>$ is the appropriate average d.p. In studying the conformation of a linear polymer in solution, it is important to start from its unperturbed dimension[31]. A linear polymer is considered as a Kuhn coil of N_s straight segments, each containing n_s monomers, such that $n_s N_s = n$, the d.p. of the

polymer. A Kuhn segment length is $I_s = n_s I_o$ where I_o is the average projection length of a monomer on the segment axis.

The root-mean-square end-to-end distance $<r_o^2>^{1/2}$ of the unperturbed coil can be then defined as

$$<r_o^2> = I_s{}^2 N_s = I_o^2 n_s n.$$

For a coil, $<r_o^2>$ is proportional to the root-mean-square radius of gyration determined by s.l.s.

$$<r_o^2> = 6<R_{Go}{}^2>.$$

However, these dimensions take into account only the short-range interactions that depend on the structure and local interactions of atoms and groups separated by only a few bonds. The long-range interactions involve pairs of chain units which are separated by many bonds and cannot occupy the same volume element at the same time. Thus, the long-range interactions are reduced to the excluded-volume effect, which increases the dimensions of the chain. The change is expressed by the semi-empirical expansion factors[25,32] α_r^2 and α_s^2 defined as

$$<r^2> = \alpha_r^2 <r_o^2>$$
$$<R_G^2> = \alpha_s^2 <R_{Go}{}^2>.$$

When the attractive forces between chain units exactly compensate their finite volume so that the effective co-volume is zero, the dimensions of the polymer are unperturbed by the excluded-volume effect. In this θ condition, $\alpha_r = \alpha_s = 1$. It follows from the theory of polymer solutions that this situation arises when the second virial coefficient A_2 is zero.

An alternative measure of chain extension is the persistence length a, introduced[33] originally in the context of the worm-like chain model and defined, for a non-free draining coil, as

$$C_\infty = \frac{2a}{I_0} - 1.$$

On the assumption that there is no preferred secondary structure, then $I_o = 0.44$ nm and $<M> = 164<n>$. The experimental values gave $C_\infty = 13.5$ and $a = 3.21$ nm for amylose in 0.1M KCl. Ring *et al.*[8] found similar values ($C_\infty = 11.7$, $a = 2.78$ nm) for the chains of polydisperse amylose in pure water with positive values of A_2. Their values were corrected for chain expansion and polydispersity, and became consistent with those of Banks and Greenwood[1] for 0.33M KCl ($C_\infty = 5.6$–5.9, $a = 1.45$–1.52 nm).

In order to calculate C_∞ for amylose in 0.1M KOH, chain expansion has to be taken into account[3]. The ratio $<R_G^2>_z/M_w$ is no longer constant, but is a continuously increasing function of the molecular weight[34]. Under these conditions, the expansion factor α_s^2 is a function of the excluded-volume parameter z:

$$\alpha_s^2 = 1 + (134/105)\, z,$$

where z is a function of $M_w^{0.5}$

$$z = \left(\frac{3}{2\pi}\right)^{\frac{3}{2}} B \left(\lim_{M\to\infty} \langle r^2\rangle_0/M\right)^{-\frac{3}{2}} M_w^{\frac{1}{2}} = c\, M_w^{\frac{1}{2}},$$

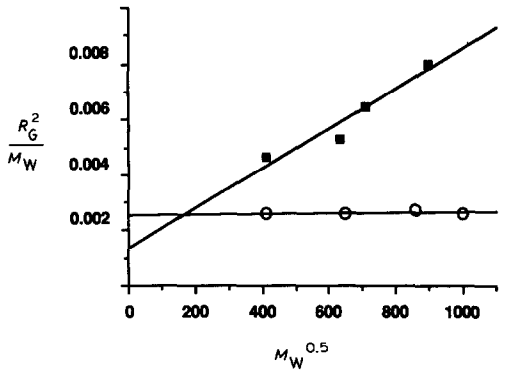

Fig. 6. Variation in R_G^2/M_w *vs.* $M_w^{0.5}$ in 0.1M KOH (■) and 0.1M KCl (o). Intercept with the ordinates gives $C_\infty l^2/6M_o$. C_∞ is the characteristic ratio, l is the projected length of the monomer unit, and M_o is the molecular weight of such a unit.

with $B = \beta/M_s^2$, where M_s is the molar mass of the segment, β is the effective volume excluded from one segment by the presence of another, and c is a constant.

Therefore R_G is increased due to the excluded-volume effect:

$<R_G^2> = \alpha_s^2 <R_{Go}^2>$.

So, $R_G^2 = \alpha_s^2 R_{Go}^2 = (1 + 134/105\, z)\, R_{Go}^2 = (1 + c'\, M_w^{0.5})\, R_{Go}^2$.

Since $R_{Go}^2 = C_\infty <n>_w l_o^2/6 = C_\infty M_w l_o^2/6M_o$, the relationship between R_G and M_w can be written as

$R_G^2/M_w = (C_\infty/6M_o) l_o^2 (1 + c'\, M_w^{0.5})$.

The variation in R_G^2/M_w versus $M_w^{0.5}$ gives, after extrapolation (Fig. 6), $C_\infty = 6.8$ and then $a = 1.71$ nm for amylose in 0.1M KOH.

With 0.1M KCl as solvent, the ratio $<R_G^2>_z/M_w$ was not dependent on the molecular weight (Fig. 6), which is further evidence that 0.1M KCl is a θ solvent at 25°. This result does not agree with the values obtained for ξ and A_2. However, Huseman *et al.*[6] pointed out that A_2 showed anomalous behaviour by increasing then decreasing with increasing molecular weight. A question arises at this point about the quality of pure water as solvent. Huseman *et al.*[6] obtained a positive value for the second virial coefficient for the enzymically synthesised amylose–water system, suggesting that water is a thermodynamically good solvent for the amylose. Ring *et al.*[8] reached the same conclusion. Our results tends to confirm that 0.1M KCl is a θ solvent, like 0.33M KCl, but further work is necessary.

Amylose chains in solution are more flexible than those of modified cellulose (cellulose diacetate $a = 4.8$–7.2 nm; carboxymethylcellulose $a = 8.0$–12.0 nm), but more rigid than those of pullulan ($a = 1.2$–1.9 nm)[35]. Therefore, all of these polysaccharides belong to the class of loosely jointed polysaccharides, in contrast to stiff polysaccharides such as xanthan ($a = 310 \pm 40$ nm) and scleroglucan ($a = 180 \pm 30$ nm)[36].

REFERENCES

1 W. Banks and C. T. Greenwood, *Starch and its Components*, Edinburgh University Press, 1975, pp. 113–190.
2 A. Guilbot and C. Mercier, in G. O. Aspinall (Ed.), *The Polysaccharides*, Vol. 3, Academic Press, London, 1985, pp. 209–285.
3 J. des Cloizeaux and G. Jannink, *Les Polymères en Solution: leur Modélisation et leur Structure*, Les Editions de Physique, Les Ulis, France, 1987, pp. 667–737.
4 W. W. Everett and J. F. Foster, *J. Am. Chem. Soc.*, 81 (1959) 3459–3464.
5 J. M. G. Cowie, *Makromol. Chem.*, 42 (1961) 230–247.
6 E. Huseman, B. Pfannemuller, and W. Burchard, *Makromol. Chem.*, 59 (1963) 1–27.
7 M. Fujita, K. Honda, and H. Fujita, *Biopolymers*, 12 (1973) 1177–1189.
8 S. G. Ring, K. J. l'Anson, and V. J. Morris, *Macromolecules*, 18 (1985) 182–188.
9 W. Banks and C. T. Greenwood, *Carbohydr. Res.*, 7 (1968) 349–356.
10 J. Hollo and J. Szejtli, in J. A. Radley (Ed.), *Starch and its Derivatives*, Chapman & Hall, London, 1968, pp. 203–246.
11 D. Braga, E. Ferracini, A. Ferrero, A. Ripamonti, D. Brant, G. S. Buliga, and A Cesaro, *Int. J. Biol. Macromol.*, 7 (1985) 161–166.
12 R. C. Jordan, D. A. Brant, and A. Cesaro, *Biopolymers*, 17 (1978) 2617–2632.
13 D. Gagnaire, S. Perez, and V. Tran, *Carbohydr. Polym.*, 2 (1982) 829–837.
14 M. J. Gidley and P. V. Bulpin, *Macromolecules*, 22 (1989) 341–346.
15 M. T. Tollier and J. P. Robin, *Ann. Technol. Agric.*, 28 (1979) 1–15.
16 D. E. Koppel, *J. Chem. Phys.*, 57 (1972) 4814–4817.
17 B. H. Zimm *J. Chem. Phys.*, 16 (1948) 1093–1099.
18 P. Colonna, V. Biton, and C. Mercier, *Carbohydr. Res.*, 137 (1985) 151–166.
19 M. B. Huglin, in M. B. Huglin (Ed.), *Light Scattering from Polymer Solution*, Academic Press, London, 1974, pp. 165–331.
20 C. T. Greenwood and D. J. Hourston, *Polymer*, 16 (1975) 474–475.
21 A. E. Hamielec and H. Meyer, in J. V. Dawkins (Ed.), *Developments in Polymer Characterization–5*, Elsevier Applied Science, Amsterdam, 1986, pp. 95–130.
22 M. Schmidt and W. Burchard, *Macromolecules*, 14 (1981) 210–211.
23 A. Z. Ackasu and C. C. Han, *Macromolecules*, 12 (1979) 276–281.
24 D. Caroline, in J. V. Dawkins (Ed.), *Developments in Polymer Characterization–5*, Elsevier Applied Science, Amsterdam, 1986, pp. 49–93.
25 P. J. Flory, *Principles of Polymer Chemistry*, Cornell University Press, Ithaca, New York, 1953, ch. X, XII, and XIV.
26 P. G. de Gennes, *Scaling Concepts in Polymer Physics*, Cornell University Press, Ithaca, New York, 1979, pp. 29–53.
27 J. C. Le Guillou and J. Zinn-Justin, *Phys. Rev. Lett.*, (1977) 95–98.
28 G. D. J. Phillies, *J. Appl. Polym. Sci.*, 43 (1989) 275–304.
29 G. Weill and J. des Cloizeaux, *J. Phys.*, 40 (1979) 99–105.
30 P. J. Flory, *Statistical Mechanics of Chain Molecules*, Interscience, New York, 1969, pp. 95–129.
31 C. Tanford, *Physical Chemistry of Macromolecules*, Wiley, New York, 1961, pp. 138–179.
32 H. Yamakawa, *Modern Theory of Polymer Solutions*, Harper and Row, New York, 1971, ch. 6.
33 O. Kratky and G. Porod, *Recl. Trav. Chim. Pays-Bas*, 68 (1949) 1106–1122.
34 M. Bohdanecky and J. Kovar, in D. Jenkins (Ed.), *Viscosity of Polymer Solutions*, Elsevier Applied Science, Amsterdam, 1982, pp. 14–22.
35 Y. Muroga, Y. Yamada, I. Noda, and M. Nagasawa, *Macromolecules*, 20 (1987) 3003–3006.
36 M. Yalpani, *Polysaccharides, Syntheses, Modifications and Structure/Property Relations*, Elsevier, Amsterdam, 1988, pp. 84–107.